HHS Public Access

Author manuscript

Mol Psychiatry. Author manuscript; available in PMC 2022 July 28.

Published in final edited form as:

Mol Psychiatry. 2022 March ; 27(3): 1542–1551. doi:10.1038/s41380-021-01422-5.

Altered canonical and striatal-frontal resting state functional connectivity in children with pathogenic variants in the Ras/mitogen-activated protein kinase pathway

Jennifer L. Bruno, PhD[*,†,1], **Sharon B. Shrestha, BA**[*,1], **Allan L. Reiss, MD**[1,2], **Manish Saggar, PhD**[1], **Tamar Green, MD**[1]

[1]Division of Interdisciplinary Brain Sciences, Department of Psychiatry and Behavioral Sciences, Stanford University School of Medicine

[2]Department of Pediatrics and Department of Radiology, Stanford University School of Medicine

Abstract

Mounting evidence supports the role of the Ras/mitogen-activated protein kinase (Ras/MAPK) pathway in neurodevelopmental disorders. Here, the authors used a genetics-first approach to examine how Ras/MAPK pathogenic variants affect the functional organization of the brain and cognitive phenotypes including weaknesses in attention and inhibition. Functional MRI was used to examine resting state functional connectivity (RSFC) in association with Ras/MAPK pathogenic variants in children with Noonan syndrome (NS). Participants (age 4–12 years) included 39 children with NS (mean age 8.44, SD=2.20, 25 females) and 49 typically developing (TD) children (mean age 9.02, SD=9.02, 33 females). Twenty-eight children in the NS group and 46 in the TD group had usable MRI data and were included in final analyses. The results indicated significant hyperconnectivity for the NS group within canonical visual, ventral attention, left frontoparietal and limbic networks ($p<0.05$ FWE). Higher connectivity within canonical left frontoparietal and limbic networks positively correlated with cognitive function within the NS but not the TD group. Further, the NS group demonstrated significant group differences in seed-based striatal-frontal connectivity ($Z>2.6$, $p<0.05$ FWE). Hyperconnectivity within canonical brain networks may represent an intermediary phenotype between Ras/MAPK pathogenic variants and cognitive phenotypes, including weaknesses in attention and inhibition. Altered striatal-frontal connectivity corresponds with smaller striatal volume and altered white matter connectivity previously documented in children with NS. These results may indicate delayed maturation and compensatory mechanisms and they are important for understanding the

† To whom correspondence should be addressed (and location where study was conducted): Department of Psychiatry and Behavioral Sciences, Stanford University 401 Quarry Road, Palo Alto, CA 94304, Phone: (818) 415-9119, Fax: (650) 724-4761, jenbruno@stanford.edu.

*Equal contribution

Author Contributions: J.L.B contributed to data analysis and interpretation and wrote the manuscript. S.B.S. contributed to data analysis and data collection. M.S. contributed to statistical methodology, data analysis and interpretation. A.L.R. contributed to data collection and interpretation. T.G. conceived and designed the study, supervised data collection, and contributed to data analysis and interpretation. All authors drafted the manuscript for intellectual content.

Disclosures: The authors report no financial relationships with commercial interests.

Supplementary information is available at MP's website

pathophysiology underlying cognitive phenotypes in NS and in the broader population of children with neurodevelopmental disorders.

The Ras/mitogen-activated protein kinase (Ras/MAPK) pathway is critical for cell cycle, growth, and differentiation and was originally identified for its role in oncogenesis.[1] More recently, converging evidence from large genome-wide association studies (GWAS) and animal models substantiates the Ras/MAPK pathway's chief role in brain development and in deviation from typical neurodevelopment.[2,3] Specific neurogenetic syndromes associated with germline mutations affecting the Ras/MAPK pathway are collectively known as RASopathies.[4] Examination of RASopathies offers a translatable approach to understanding the Ras/MAPK pathway's effects on typical and atypical human brain development. RASopathies can play a unique role in unraveling complex genetic and neurobiological factors and could eventually facilitate development of therapies targeting underlying causal mechanisms in neurodevelopmental disorders.[5] A genetics-first approach aimed at identifying causal mechanisms and targets for therapy is urgently needed to advance treatment approaches for neurodevelopmental disorders. For example, the current standard of treatment for attention-deficit hyperactivity disorder (ADHD), one of the most prevalent neurodevelopmental disorders, is primarily stimulants. Yet, stimulants are only effective at reducing symptoms in the short term and do not address underlying mechanisms.[6]

Noonan syndrome (NS, 1:2000), the most common RASopathy,[7] is associated with a diverse phenotype including short stature, congenital heart defects, ADHD,[8,9] learning disabilities, and autism spectrum disorder (ASD) symptoms.[10,11] Over ~65% of individuals with NS present with missence mutations of *PTPN11* or *SOS1* genes[12] (Figure 1). PTPN11 and *SOS1* pathogenic variants lead to downstream upregulation of the RAS/MAPK signaling cascade[12–14]. In particular, *PTPN11* encodes Shp-2, a major regulatory protein tyronsine phosphatase in the RAS/MAPK pathway. Most *PTPN11* pathogenic variants are associated with altered amino-terminal src-homology 2 (N-SH2)/protein tyrosine phosphatase (PTP) interactions that stabilize Shp-2 protein in the active conformation[15]. The active conformation of Shp-2 in turn leads to RAS/MAPK pathway upregulation.[7,13] In the animal model, pathogenic variants of *PTPN11* that affect Shp-2 are associated with reduced axon myelination and increased excitatory synaptic function.[16] Induced pluripotent stem cells derived from individuals with NS related pathogenic variants in PTPN11 demonstrates precocious development of glial cells.[17] The *SOS1* gene encodes a guanine nucleotide exchange factor (GEF) that activates Ras and downstream Ras/MAPK signaling; *SOS1* gain-of-function pathogenic variants diminish SOS1 protein autoregulation and enhance Ras/MAPK signaling.[12] Thus, in the context of NS, both *PTPN11* and *SOS1* pathogenic variants are associated with Ras/MAPK pathway gain-of-function. The effects of RAS-MAPK pathway gain of function on the brain are also evidenced by pathogenic variants downstream of *PTPN11* and *SOS1.* For example, in the mouse model, deletion of the Map 2k1/Mek1 and Map2k2/Mek2 kinases leads to inactivation of the Ras-MAPK pathway and disrupts the elongation of corticospinal axons[18]. Further, data from fruit fly and zebrafish indicates that, depending upon the cellular context, pathogenic variants in] Map2k2 gene (encoding MEK) can increase or decrease Ras-MAPK activation.[19]

Mounting evidence supports the consideration of NS and its effects on the Ras/MAPK pathway as a human model system for understanding genetic and neurobiological substrates of neurodevelopmental disorders, specifically ADHD. First, our lab and others have demonstrated that children with NS are at significantly increased risk (38–49% in NS[10,11] vs 11% of children in the general population[20]) for ADHD diagnosis. Second, children with NS present with reduced volumes of the striatum,[21,22] a brain region implicated in attention and hyperactivity, core symptoms of ADHD.[23] Third, 20% of children with idiopathic ADHD demonstrate pathogenic variants within the metabotropic glutamatergic network (mGluR) network, which regulates Ras/MAPK signaling.[24] Finally, gene discovery in idiopathic neurodevelopmental disorders indicates that the encoded proteins of varied genes cluster within the Ras/MAPK signaling pathway suggesting that neurodevelopmental disorders are associated with enrichment of Ras/MAPK signaling.[3]

The aforementioned research demonstrates that Ras/MAPK pathway alterations play a critical role in human brain structure and white matter connectivity and are associated with increased risk for ADHD symptoms. However, the effects of NS-specific Ras/MAPK pathway pathogenic variants on functional brain organization are unknown. The rationale for investigating functional connectivity in NS is supported by the following evidence. First, functional connectivity is strongly tied to underlying white matter connectivity and white matter connectivity is altered in NS.[25] Second, evidence from another RASopathy, neurofibromatosis 1 (NF1), indicates a link between Ras/MAPK pathway pathogenic variants and altered functional connectivity.[26,27] Finally, resting state functional connectivity (RSFC) may play a unique role in understanding the functional pathophysiology underlying ADHD symptoms in NS. RSFC quantifies intrinsic, spontaneous co-fluctuations across brain regions not related to an explicit task[28,29] and is applicable across wide age ranges and levels of cognitive functioning.[29]

We hypothesized that functional connectivity patterns are altered in children with NS relative to an age and sex matched group of typically developing children (TD). As the present study represents the first investigation of RSFC in NS we examined differences in whole-brain functional organization within well-established canonical resting state networks (RSNs)[30] using data-driven independent component analysis (ICA). Secondarily, we examined connectivity patterns involving bilateral striatum (caudate and putamen)[21] using seed-based analyses.

Methods

Participants

Participants (age 4–12 years) included 39 children with NS (mean age=8.44, SD=2.20, 25 females) and 49 TD children (mean age=9.02, SD=9.02, 33 females). Given that this is the first study examining RSFC in children with NS, we estimated power based on our structural data (*SOS1* d=−0.9 and *PTPN11* d=−1.5 compared to TD children). Using a more conservative Cohen's d value, the estimated power to detect differences between the groups is 0.83 for a cohort of 28 (size of our NS group after data scrubbing, see Image acquisition and preprocessing section below).

Participants with NS presented results from genetic testing confirming the presence of *PTPN11* (N=29) or *SOS1* (N=10) pathogenic variants. Research was performed at the Stanford University School of Medicine and the Institutional Review Board approved all study procedures. Written, informed consent was obtained from a legal guardian for all participants. All participants over 7 years provided assent. Recruitment strategy and exclusionary criteria are detailed in the Supplementary Methods.

We examined children pre- or in early stages of puberty to avoid influence of pubertal effects on the brain. Pubertal status was assessed by an experienced physician using Tanner staging.[31,32] Parental report of Tanner stage was used for 4 participants in the TD group for which physician examination was not available. Participants completed age-appropriate versions of the Wechsler Intelligence Scale[33,34] and select subtests from A Developmental NEuroPSYchological Assessment (NEPSY-II, Table 1).[35]

Image acquisition and preprocessing

All participants completed behavioral training in a mock MRI scanner to reduce sensitivity to the MRI environment and to reduce motion during the actual scan.[36] Imaging protocols and preprocessing are described in the Supplementary Methods.

Data was scrubbed or censured using the following procedures. Each frame with displacement>0.5mm was removed in addition to one frame immediately prior to and two frames immediately following that frame to reduce the impact of head movement artifacts.[37] At the participant level, imaging data were included in the analysis if they met the following criteria 1) structural and functional scans were of sufficient quality and sufficiently similar in orientation to pass registration procedures as defined by FMRIPrep (https://fmriprep.org/en/1.0.3/api/index.html), 2) ≥4 min of artifact-free functional data was available after scrubbing as defined above. Within the NS group 11 out of 39 (28%) participants were excluded based on these criteria. Within the TD group 3 out of 16 (19%) individuals were excluded and 33 TD individuals were included from larger studies which reported 6 out of 39 excluded (15%).[38] Group-wise analyses included 28 NS and 46 TD individuals (see Table 1). Groups were not different in terms of number of scrubbed frames or duration of clean resting-state data (Table 1).

Connectivity within canonical resting state networks

We used independent component analysis (ICA) and dual-regression to examine group differences in connectivity within canonical RSNs.[39] First, we ran group-based ICA using melodic v3.15 to produce RSNs across the cohort without over-representing one group. A subgroup of 28 participants from the TD group was selected to ensure equal group size for ICA. TD children were chosen individually to create the subgroup that most closely matched the NS group for age, sex and Tanner stage. Group ICA resulted in 60 components. We then compared each component to canonical RSNs[30] using spatial correlation (FSLCC). We chose among components those whose spatial maps most closely matched canonical RSNs[30] based on visual inspection and spatial correlation: visual (r=0.514), somatomotor (two individual components combined for spatial correlation and further analysis (r=0.551)), dorsal attention (r=0.413), ventral attention (r=0.411), limbic (r=0.574), left frontoparietal

(r=0.219), right frontoparietal (r=0.449), default mode (r=0.271). We used dual regression to estimate individual maps representing participant-specific versions of each network for all participants (i.e., 28 NS and 46 TD).[40] Each map was used as a participant-level contrast and group differences were estimated using the *randomise* tool with threshold-free cluster enhancement including age and sex as covariates of no interest.[41] Randomise is a non-parametric permutation testing method that does not require assumptions of data normality to be met. For robust results, we used 10,000 permutations, $p<0.05$ FWE and # voxels > 26 for cluster identification. FDR correction was used to control for multiple comparisons across the eight networks.

Seed-based striatal connectivity

We examined whole brain connectivity using caudate and putamen as seeds. First, we created anatomical masks for each left and right caudate and putamen using the Harvard-Oxford subcortical atlas in FSLeyes. Each mask was eroded to include 75% of the original voxels and ensure overlap with each participant's standard space image. This procedure resulted in the following ROI sizes (in voxels): left caudate: 234, right caudate: 239, left putamen: 488, right putamen: 481. We used fMRI Expert Analysis Tool (FEAT)[42] to model extracted time series from ROIs in conjunction with all other grey matter voxels in the brain. First level and group level statistics were performed using robust nonparametric methods in FEAT. Group level statistics were performed with age and sex as covariates of no interest and cluster correction ($Z=2.6$, $p<0.05$ FWE). Comparisons for each seed were considered significant if they passed FDR correction across the four seeds.

Post hoc correlations

We examined relationships between connectivity (from ICA) and performance on the NEPSY-II. We did not examine correlations with our secondary (seed-based) analysis to limit the number of statistical tests. Principal components analysis (PCA) was performed for data reduction across all participants using all available NEPSY-II data (22 subtest scores, Table 1*.)* using the *prcomp* function in R. This approach limits the number of comparisons and avoids overfitting and limited generalizability associated with correlations using only one metric.[43] Participants <7 years old were excluded due to not completing all NEPSY-II measures (some subtests are only appropriate for age >/=7). A small percentage of subtest data was missing for participants over age 7 (1.5% across participants and subtests). Prior to PCA we performed data imputation (N=20 imputations) using a predictive mean matching for mixed types and the *Multiple Imputation by Chained Equations* (MICE) package in R.

We performed Pearson's correlation between network connectivity values and PCA-derived NEPSY-II components (two-tailed significance is reported). Fisher's transformation was used to convert r values to Z scores which were compared to assess between-group differences in relationship strength.

PTPN11 subgroup analysis

Group level comparisons were repeated for the *PTPN11* subgroup (N=21) and the full TD group. Brain/behavior relationships were also investigated within the *PTPN11* subgroup.

The *SOS1* subgroup was too small to warrant statistical comparison (N=10). Effect sizes were calculated for each genetic subgroup (*PTPN11* and *SOS1*).

Results

NS and TD groups did not differ in age, sex or Tanner stage (all p's >0.09, Table 1). The NS group demonstrated lower full-scale IQ and lower scores for most NEPSY-II subtests (Table 1).

ICA demonstrated significant hyperconnectivity for the NS group relative to the TD group for four of eight canonical RSNs: visual, ventral attention, left frontoparietal and limbic ($p<0.05$ FEW, Figure 1, Table 2).

Seed-based analysis indicated significant group differences in RSFC. Bilaterally, the caudate seed demonstrated hyperconnectivity with contralateral prefrontal cortex in the NS group (relative to TD). However, the left caudate seed demonstrated hypoconnectivity with the ipsilateral (left) dorsolateral prefrontal cortex (DLPFC) in the NS group (relative to TD). Hypoconnectivity was also observed in the NS group (relative to TD) between the left putamen and somatosensory regions as well as between the right putamen and thalamus (Figure 2, Table 2).

To examine the brain-behavior associations, we correlated connectivity estimates with components from NEPSY-II PCA. PCA reduced NEPSY-II data into 3 components while accounting for 49.5% of the variance (Figure 3). Rotation values were used to interpret each component. The first component (accounting for 30.1% of the variance) represented roughly equal contribution across NEPSY-II scores and was strongly correlated with IQ ($r(57) = -0.790$, $p<0.0001$, IQ was not entered into PCA analysis). This general component was not used for further correlation as our goal was to examine relationships with distinct NEPSY-II processes. The second component (11.6% variance) was driven primarily by memory and the third (7.8% variance) was driven primarily by inhibition and motor. The memory and the inhibition/motor components were not correlated with IQ (p's>0.10). Within the NS group the inhibition/motor component was significantly related to connectivity within with left frontoparietal and limbic clusters ($p<0.05$, Table 2, Figure 3). These relationships were not significant within the TD group ($p>0.10$). The group difference (NS vs. TD) in correlation strength was significant for frontoparietal and limbic and clusters (p's<0.05). Correlations between the memory component and network connectivity were not significant within either group (p's >0.10)

Subgroup ICA results indicated significant hyperconnectivity for the *PTPN11* subgroup within visual, ventral attention, left frontoparietal and limbic networks with significant overlap with the primary results (Table S1). Seed-based results demonstrate correspondence with the primary results (Table S1) and differences include lack of hyperconnectivity between right caudate and left frontal cortex and lack of hypoconnectivity between right putamen and subcortical regions for the *PTPN11* subgroup. However, subgroup analysis did reveal a cluster demonstrating hypoconnectivity between right caudate and left anterior cingulate cortex. We also reexamined subgroup results at a more relaxed threshold (Z=1.7)

which, in addition to the clusters reported in Table S1, revealed hyperconnectivity between right caudate and left frontal cortex as well as hypoconnectivity between right putamen and left thalamus. Significant correlations within the *PTPN11* subgroup also corresponded to those identified in the primary analysis (Table S1).

Effect sizes for *PTPN11* (N=21 after data censuring) and *SOS1* (N=7 after data censuring) subgroups demonstrated similar patterns of results (compared to the primary analysis) relative to TD (Table 2). Effect sizes were calculated for each of the significant peaks identified in the primary results (Table 2).

Discussion

This study presents the first evidence of altered functional brain organization in children with NS and the first data-driven (ICA) investigation of RSFC within the broader RASopathies. Hyperconnectivity within visual, ventral attention, left frontoparietal and limbic networks (four out of eight networks tested) may reflect a widespread neurophenotype related to Ras/MAPK pathway over-activation.[15] Altered caudate/frontal cortex connectivity includes contralateral hyperconnectivity and ipsilateral hypoconnectivity and may reflect a compensatory shift in striatal-frontal connectivity due to underlying anatomical differences.[21,22] Relationships between ICA-based connectivity levels and inhibition/motor skills, some of the most impaired cognitive skills among this cohort, suggest that altered connectivity with canonical RSNs may underlie deficits in these domains. Further, these results lend support to conceptualizing RSFC as an intermediary phenotype between altered Ras/MAPK function and the NS cognitive phenotype.

The data-driven ICA results indicated hyperconnectivity within visual, ventral attention, left frontoparietal and limbic networks with no evidence of hypoconnectivity. The ventral attention network is involved with detection and orienting to unexpected but behaviorally relevant stimuli.[44,45] Further, the ventral network is linked to the visual network via its role in visual spatial processing.[45] The frontoparietal network is key for spatial attention and working memory.[46] Thus, our results support the hypothesis that NS is associated with hyperconnectivity across a diverse group of networks, which are responsible for processes underlying a range of attention and orientation abilities.[44]

This first application of ICA in a RASopathy presents novel evidence of the Ras/MAPK pathway's effect on large scale networks. While the link between synaptic plasticity and brain network connectivity is not yet fully understood, emerging evidence from Alzheimer's disease and schizophrenia indicates that synaptic plasticity dysfunction may drive brain network dysfunction[47]. Further, evidence supports the link between synaptic plasticity disfunction, as seen in the mouse model of NS,[16,48] and aberrant network connectivity. First, impaired synaptic plasticity can influence the synchrony of local and distributed neuronal oscillations which in turn interrupts overall network connectivity[49,50]. Second, long term potentiation (LTP), a specific type of plasticity underlying learning and memory that is impaired in NS[16,48], may form the basis of network organization[47]. Impaired LTP may disrupt connectivity in a way that reduces overall efficiency, thus ICA-based hyperconnectivity in NS may reflect a maladaptive upscaling of network activity in response

inefficiency.[47] Finally, increases in functional brain connectivity are commonly seen after brain injury[51,52]. Thus, increased connectivity in NS may reflect a compensatory response to aberrant white matter pathology evidenced by reduced axon myelination in the mouse model [16] and less efficient white matter connectivity in humans[22].

Higher within-network connectivity in NS may also indicate delayed maturation of brain networks as previous studies in typically-developing individuals have indicated that within-network connectivity weakens with age while between-network connectivity strenthens.[53,54] Longitudinal studies in NS will be required to fully understand the pattern of network changes but this intriguing hypothesis is supported somewhat by previous research suggesting that the cognitive performance discrepancy in NS decreases with age.[55] Further, adults with NS show no deficit across several cognitive domains including executive function.[56]

For the NS group, connectivity within the left frontoparietal and limbic networks was positively associated with the inhibition/motor component derived from NEPSY-II scores. The inhibition/motor component was negatively correlated with *Response Set* and *Fingertip Tapping (nondominant hand)*, indicating that higher scores on this component are associated with lower performance on inhibition and motor tasks. Further, this component was not related to IQ, indicating specificity for these relationships between connectivity and inhibition/motor skills. Thus, hyperconnectivity in left frontoparietal and limbic networks may reflect a maladaptive reorganization of connectivity whereby children with NS who have inferior inhibition and motor performance have increased connectivity. Our previous work provides further evidence linking connectivity (white matter fiber tract integrity) with individual inhibition and motor measures of the NEPSY-II.[22] The current study's use of PCA to reduce NEPSY-II data to a small number of components represents a methodological advancement that avoids overfitting and has improved generalizability when compared to methods examining relationships with individual cognitive scores.[43]

Functional connectivity correlates strongly with underlying anatomical connectivity in human neuroimaging[25,57] and animal studies.[58] Accordingly, our present results demonstrate a pattern of altered seed-based functional connectivity that maps onto anatomical differences we previously identified in NS.[21,22] In particular, our previous work revealed lower grey matter volume for caudate, decreased cortical thickness for right DLPFC,[21] and lower fiber integrity for striatal tracts.[22] Our seed-based results indicated hyperconnectivity between left caudate and right anterior cingulate as well as hyperconnectivity between right caudate and left inferior frontal gyrus (IFG) for children with NS. Conversely, left caudate demonstrated hypoconnectivity with left IFG and dorsolateral prefrontal cortex (DLPFC). This combination of hyper- and hypoconnectivity indicates a shift in balance of striatal-frontal connectivity that may reflect compensation related to altered neuroanatomy in children with NS. Finally, hypoconnectivity between the left caudate and motor regions as well as between bilateral thalamus and sensory motor regions may also be related to altered structure of these particular striatal regions and their associated white matter tracts.[21,22]

The seed-based results are consistent with previous evidence from NF1 suggesting potential common effects of Ras/MAPK pathway gain-of-function. First, combined animal and human evidence indicates a shift in balance of connectivity including striatal dysfunction, increased limbic and decreased frontoparietal connectivity.[59] The NF1 (*Plp-Nf1*$^{fl/+}$) mouse model also demonstrates reduced functional connectivity involving somatomotor cortex and altered underlying white matter.[60] Human resting state studies further indicate reduced connectivity for anterior-posterior connections[26] and reduced caudate/frontal cortex connectivity in NF1.[61] The present study found a combination of hyper- and hypoconnectivity, a pattern found in only one of the previous NF1 studies.[27] Given the significant differences in methodology and clinical focus, we are not yet able to define the correspondence between altered patterns of brain function in NS and NF1. Importantly, both behavioral[62] and pharmacological[63] treatments may alter RSFC patterns associated with Ras/MAPK pathway disruptions in NF1. This knowledge combined with the present RSFC differences in NS suggests that functional connectivity could be used as a relevant biomarker in children with RASopathies, specifically NS and NF1. However, pathogenic variants of *PTPN11* and *SOS1* modulate multiple pathways in addition to Ras/MAPK including phosphoinositide 3-kinase (PI3K)/AKT [64,65]. Shp-2, the encoded protein of *PTPN11* also plays a modulatory role in the protein kinase C (PKC) pathway[66]. In the case of *PTPN11* gene, the impact of multiple pathway dysregulation may be responsible for the wide variability of phenotypic presentation including characteristics not classically associated with NS such as deep set eyes and delayed tooth eruption[67]. Thus, consideration of multiple pathways affected by NS-causing pathogenic variants and multiple treatment targets will be important for assessing the efficacy of pharmacological treatments aimed at correcting aberrant signal transduction.

Our primary results describe altered RSFC in children with NS including *PTPN11* and *SOS1* pathogenic variants. Both *PTPN11* and *SOS1* subgroups demonstrated effect sizes (relative to TD) that were comparable to our primary results (Table 2). We performed additional analyses within the PTPN11 subgroup revealing largely the same pattern of hyper and hypoconnectivity as our primary results (Table S1). Notable differences include lack of significant left caudate-bilateral premotor hyperconnectivity and lack of right putamen-thalamus hypoconnectivity in the *PTPN11* subgroup. Reduced threshold exploratory subgroup analyses indicated that the aforementioned absent hyper- and hypoconnectivity patterns were present in the *PTPN11* subgroup and lack of results at our more conservative threshold was due to limited power. Unfortunately, our sample of children with *SOS1* pathogenic variants was too small for statistical comparison (N=7 after data censuring). Larger follow-up studies with adequate sample sizes of both pathogenic variants will be informative for understanding the unique pathophysiology associated with specific pathogenic variants affecting Ras/MAPK function.

Our rigorous data censoring was necessary to ensure head motion and other artifacts did not influence results, yet it reduced our sample size. In particular, our sample size is limited for examining brain/behavior relationships. However, we present the first investigation of relatively rare pathogenic variants with a known large effect on brain structure.[21,22] Furthermore, we examined relationships within a limited set of hypothesis-driven brain regions and cognitive domains, further reduced via PCA. Several studies have indicated

patterns of hyper and hypo-connectivity in association with idiopathic ADHD, which partly overlap with the results of the present study,[68,69] yet a recent meta-analysis demonstrated lack of spatial convergence across studies potentially owing to the heterogeneity with ADHD pathophysiology.[69] Thus, studies examining connectivity in more homogeneous clinical groups such as NS play a special role in understanding ADHD pathophysiology and hold potential for informing future observational and treatment studies. Replication of findings and examination of longitudinal connectivity changes will be essential for further interpretation.

Together our results describe a pattern of hyperconnectivity within canonical resting state networks and compensatory (hyper- and hypo-) striatal-frontal connectivity. This pattern of altered connectivity may represent an intermediary phenotype between Ras/MAPK gain of function and cognitive phenotypes in NS. Correlations between connectivity and cognitive functioning in the NS group suggest that connectivity changes may directly underlie some of the cognitive deficits in affected children. These results, including putative evidence of delayed maturation (as evidenced by hyperconnectivity)[53,54] and compensatory mechanisms, are important for understanding the pathophysiology underlying ADHD symptoms in NS and they may have utility in identifying pathophysiology in subgroups within idiopathic ADHD. Additionally, these findings suggest that RSFC may be a relevant biomarker to facilitate planning targeted therapies and/or for monitoring response to treatment with already available drugs that alter signaling in the Ras/MAPK pathway (i.e. MEK inhibitors).[70] Finally, our results provide essential data on brain function in rare genetic condition affecting the Ras/MAPK pathway.

Data availability:

The final dataset will be stripped of all identifiers and made available to qualified investigators upon request.

Supplementary Material

Refer to Web version on PubMed Central for supplementary material.

Acknowledgements:

This work was supported by the National Institute of Child Health and Human Development (#HD090209 K23). The typically developing participants in this study were recruited through work that was supported by a grant from the National Institute of Mental Health (#MH099630). T.G was also supported by The Francis S. Collins Scholar in Neurofibromatosis Clinical and Translational Research. M.S. was supported by a NIH Director's New Innovator Award (MH119735 DP2) and a Faculty Scholar Award from the Stanford Maternal and Child Health Research Institute.

We gratefully acknowledge the support of The Lucas Service Center at Stanford, and the families who participated in this research.

References

1. Bos JL. Ras Oncogenes in Human Cancer: A Review. Cancer Res 1989; 49: 4682–4689. [PubMed: 2547513]

2. Gandal MJ, Haney JR, Parikshak NN, Leppa V, Ramaswami G, Hartl C et al. Shared molecular neuropathology across major psychiatric disorders parallels polygenic overlap. Science (80-) 2018; 359: 693–697.

3. Moyses-Oliveira M, Yadav R, Erdin S, Talkowski ME. New gene discoveries highlight functional convergence in autism and related neurodevelopmental disorders. Curr Opin Genet Dev 2020; 65: 195–206. [PubMed: 32846283]

4. Tidyman WE, Rauen KA. The RASopathies: developmental syndromes of Ras/MAPK pathway dysregulation. Curr Opin Genet Dev 2009; 19: 230–236. [PubMed: 19467855]

5. Sanders SJ, Sahin M, Hostyk J, Thurm A, Jacquemont S, Avillach P et al. A framework for the investigation of rare genetic disorders in neuropsychiatry. Nat Med 2019; 25: 1477–1487. [PubMed: 31548702]

6. Caye A, Swanson JM, Coghill D, Rohde LA. Treatment strategies for ADHD: an evidence-based guide to select optimal treatment. Mol Psychiatry 2019; 24: 390–408. [PubMed: 29955166]

7. Tartaglia M, Gelb BD, Zenker M. Noonan syndrome and clinically related disorders. Best Pract Res Clin Endocrinol Metab 2011; 25: 161–179. [PubMed: 21396583]

8. Pierpont EI, Hudock RL, Foy AM, Semrud-Clikeman M, Pierpont ME, Berry SA et al. Social skills in children with RASopathies: A comparison of Noonan syndrome and neurofibromatosis type 1. J Neurodev Disord 2018; 10: 1–11. [PubMed: 29329511]

9. Alfieri P, Piccini G, Caciolo C, Perrino F, Gambardella ML, Mallardi M et al. Behavioral Profile in RASopathies. Am J Med Genet Part A 2014; 164: 934–942.

10. Green T, Naylor PE, Davies W. Attention deficit hyperactivity disorder (ADHD) in phenotypically similar neurogenetic conditions: Turner syndrome and the RASopathies. J Neurodev Disord 2017; 9: 1–12. [PubMed: 28115995]

11. Pierpont EI, Tworog-Dube E, Roberts AE. Attention skills and executive functioning in children with Noonan syndrome and their unaffected siblings. Dev Med Child Neurol 2014; 57: 385–392. [PubMed: 25366258]

12. Tartaglia M, Pennacchio LA, Zhao C, Yadav KK, Fodale V, Sarkozy A et al. Gain-of-function SOS1 mutations cause a distinctive form of Noonan syndrome. Nat Genet 2007; 39: 75–79. [PubMed: 17143282]

13. Bunda S, Burrell K, Heir P, Zeng L, Alamsahebpour A, Kano Y et al. Inhibition of SHP2-mediated dephosphorylation of Ras suppresses oncogenesis. Nat Commun 2015; 6. doi:10.1038/ncomms9859.

14. Roberts AE, Araki T, Swanson KD, Montgomery KT, Schiripo TA, Joshi VA et al. Germline gain-of-function mutations in SOS1 cause Noonan syndrome. Nat Genet 2007; 39: 70–74. [PubMed: 17143285]

15. Tartaglia M, Kalidas K, Shaw A, Song X, Musat DL, Van der Burgt I et al. PTPN11 mutations in noonan syndrome: Molecular spectrum, genotype-phenotype correlation, and phenotypic heterogeneity. Am J Hum Genet 2002; 70: 1555–1563. [PubMed: 11992261]

16. Lee Y-S, Ehninger D, Zhou M, Oh J-Y, Kang M, Kwak C et al. Mechanism and treatment for learning and memory deficits in mouse models of Noonan syndrome. Nat Neurosci 2014; 17: 1736–1743. [PubMed: 25383899]

17. Ju Y, Park JS, Kim D, Kim B, Lee JH, Nam Y et al. SHP2 mutations induce precocious gliogenesis of Noonan syndrome-derived iPSCs during neural development in vitro. Stem Cell Res Ther 2020; 11: 1–19. [PubMed: 31900237]

18. Xing L, Larsen RS, Bjorklund GR, Li X, Wu Y, Philpot BD et al. Layer specific and general requirements for ERK/MAPK signaling in the developing neocortex. Elife 2016; 5: 1–29.

19. Goyal Y, Jindal GA, Pelliccia JL, Yamaya K, Yeung E, Futran AS et al. Divergent effects of intrinsically active MEK variants on developmental Ras signaling. Nat Genet 2017; 49: 465–469. [PubMed: 28166211]

20. Attention-Deficit/Hyperactivity Disorder (ADHD) Statistics. Natl. Instiute Ment. Heal. https://www.nimh.nih.gov/health/statistics/attention-deficit-hyperactivity-disorder-adhd.

21. Johnson EM, Ishak AD, Naylor PE, Stevenson DA, Reiss AL, Green T. PTPN11 Gain-of-Function Mutations Affect the Developing Human Brain, Memory, and Attention. Cereb Cortex 2019; 29: 2915–2923. [PubMed: 30059958]

22. Fattah M, Raman MM, Reiss AL, Green T. PTPN11 Mutations in the Ras-MAPK Signaling Pathway Affect Human White Matter Microstructure. Cereb Cortex 2021; 31: 1489–1499. [PubMed: 33119062]
23. Oldehinkel M, Beckmann CF, Pruim RHR, Franke B, Hartman CA, Hoekstra PJ et al. Attention-Deficit/Hyperactivity Disorder symptoms coincide with altered striatal connectivity. 2016; 1: 353–363.
24. Elia J, Ungal G, Kao C, Ambrosini A, De Jesus-Rosario N, Larsen L et al. Fasoracetam in adolescents with ADHD and glutamatergic gene network variants disrupting mGluR neurotransmitter signaling. Nat Commun 2018; 9. doi:10.1038/s41467-017-02244-2.
25. Honey CJ, Sporns O, Cammoun L, Gigandet X, Thiran JP, Meuli R et al. Predicting human resting-state functional connectivity from structural connectivity. Proc Natl Acad Sci U S A 2009; 106: 2035–2040. [PubMed: 19188601]
26. Tomson SN, Schreiner MJ, Narayan M, Rosser T, Enrique N, Silva AJ et al. Resting state functional MRI reveals abnormal network connectivity in neurofibromatosis 1. Hum Brain Mapp 2015; 36: 4566–4581. [PubMed: 26304096]
27. Shofty B, Bergmann E, Zur G, Asleh J, Bosak N, Castellanos FX et al. Autism-associated Nf1 deficiency disrupts corticocortical and corticostriatal functional connectivity in human and mouse. 2019; : 1–28.
28. Kelly C, Biswal B, Craddock RC, Castellanos FX, Milham MP. Characterizing variation in the functional connectome: promise and pitfalls. 2012; 16: 1–16.
29. Castellanos FX, Aoki Y. Intrinsic Functional Connectivity in Attention-Deficit/ Hyperactivity Disorder: A Science in Development. Biol Psychiatry Cogn Neurosci Neuroimaging 2016; 1: 253–261. [PubMed: 27713929]
30. Yeo BT, Krienen FM, Sepulcre J, Sabuncu MR, Lashkari D, Hollinshead M et al. The organization of the human cerebral cortex estimated by intrinsic functional connectivity. J Neurophysiol 2011; 106: 1125–1165. [PubMed: 21653723]
31. Marshall WA, Tanner JM. Variations in pattern of pubertal changes in boys. Obstet Gynecol Surv 1970; 45: 13–23.
32. Marshall WA, Tanner JM. Variations in pattern of pubertal changes in girls. Arch Dis Child 1969; 44: 291–303. [PubMed: 5785179]
33. Wechsler D Wechsler intelligence scale for children–Fourth Edition (WISC-IV). San Antonio 2003.
34. Wechsler D Wechsler Preschool and Primary Scale of Intelligence. Wechsler Presch Prim Scale Intell 2002; : 120–130.
35. Brooks BL, Sherman EMS, Strauss E. NEPSY-II: A Developmental Neuropsychological Assessment, Second Edition. Child Neuropsychol 2009; 16: 80–101.
36. Barnea-Goraly N, Weinzimer SA, Ruedy KJ, Mauras N, Beck RW, Marzelli MJ et al. High success rates of sedation-free brain MRI scanning in young children using simple subject preparation protocols with and without a commercial mock scanner-the Diabetes Research in Children Network (DirecNet) experience. Pediatr Radiol 2014; 44: 181–186. [PubMed: 24096802]
37. Power JD, Schlaggar BL, Petersen SE. Recent progress and outstanding issues in motion correction in resting state fMRI. Neuroimage 2015; 105: 536–551. [PubMed: 25462692]
38. Green T, Saggar M, Ishak A, Hong DS, Reiss AL. X-Chromosome Effects on Attention Networks: Insights from Imaging Resting-State Networks in Turner Syndrome. Cereb Cortex 2018; 28: 3176–3183. [PubMed: 28981595]
39. Filippini N, MacIntosh BJ, Hough MG, Goodwin GM, Frisoni GB, Smith SM et al. Distinct patterns of brain activity in young carriers of the APOE-epsilon4 allele. Pnas 2009; 106: 7209–7214. [PubMed: 19357304]
40. Nickerson LD, Smith SM, Öngür D, Beckmann CF. Using dual regression to investigate network shape and amplitude in functional connectivity analyses. Front Neurosci 2017; 11: 1–18. [PubMed: 28154520]
41. Winkler AM, Ridgway GR, Webster MA, Smith SM, Nichols TE. Permutation inference for the general linear model. Neuroimage 2014; 92: 381–397. [PubMed: 24530839]

42. Beckmann CF, Jenkinson M, Smith SM. General multilevel linear modeling for group analysis in FMRI. Neuroimage 2003; 20: 1052–1063. [PubMed: 14568475]
43. Shen X, Finn ES, Scheinost D, Rosenberg MD, Chun MM, Papademetris X et al. Using connectome-based predictive modeling to predict individual behavior from brain connectivity. Nat Protoc 2017; 12: 506–518. [PubMed: 28182017]
44. Peterson SE, Posner MI. The Attention System of the Human Brain: 20 Years After. Annu Rev Neurosci 2012; 21: 73–89.
45. Vossel S, Geng JJ, Fink GR. Dorsal and ventral attention systems: Distinct neural circuits but collaborative roles. Neuroscientist 2014; 20: 150–159. [PubMed: 23835449]
46. Ptak R, Schnider A, Fellrath J. The Dorsal Frontoparietal Network: A Core System for Emulated Action. Trends Cogn Sci 2017; 21: 589–599. [PubMed: 28578977]
47. Bassi MS, Iezzi E, Gilio L, Centonze D, Buttari F. Synaptic plasticity shapes brain connectivity: Implications for network topology. Int J Mol Sci 2019; 20. doi:10.3390/ijms20246193.
48. Ryu HH, Kim TH, Kim JW, Kang M, Park P, Kim YG et al. Excitatory neuron–specific SHP2-ERK signaling network regulates synaptic plasticity and memory. Sci Signal 2019; 12: 1–14.
49. Uhlhaas PJ, Singer W. Abnormal neural oscillations and synchrony in schizophrenia. Nat Rev Neurosci 2010; 11: 100–113. [PubMed: 20087360]
50. Uhlhaas PJ, Singer W. Neural Synchrony in Brain Disorders: Relevance for Cognitive Dysfunctions and Pathophysiology. Neuron 2006; 52: 155–168. [PubMed: 17015233]
51. Iraji A, Benson RR, Welch RD, O'Neil BJ, Woodard JL, Ayaz SI et al. Resting State Functional Connectivity in Mild Traumatic Brain Injury at the Acute Stage: Independent Component and Seed-Based Analyses. J Neurotrauma 2015; 32: 1031–1045. [PubMed: 25285363]
52. Hillary FG, Rajtmajer SM, Roman CA, Medaglia JD, Slocomb-Dluzen JE, Calhoun VD et al. The rich get richer: Brain injury elicits hyperconnectivity in core subnetworks. PLoS One 2014; 9. doi:10.1371/journal.pone.0104021.
53. Rubinov M, Sporns O. Complex network measures of brain connectivity: uses and interpretations. Neuroimage 2010; 52: 1059–69. [PubMed: 19819337]
54. Lopez KC, Kandala S, Marek S, Barch DM. Development of Network Topology and Functional Connectivity of the Prefrontal Cortex. Cereb Cortex 2020; 30: 2489–2505. [PubMed: 31808790]
55. Roelofs RL, Janssen N, Wingbermühle E, Kessels RPC, Egger JIM. Intellectual development in Noonan syndrome: a longitudinal study. Brain Behav 2016; 6: 1–8.
56. Wingbermühle E, Roelofs RL, van der Burgt I, Souren PM, Verhoeven WMA, Kessels RPC et al. Cognitive functioning of adults with Noonan syndrome: a case-control study. Genes, Brain Behav 2012; 11: 785–793. [PubMed: 22783933]
57. Damoiseaux JS, Greicius MD. Greater than the sum of its parts: A review of studies combining structural connectivity and resting-state functional connectivity. Brain Struct Funct 2009; 213: 525–533. [PubMed: 19565262]
58. Grandjean J, Zerbi V, Balsters JH, Wenderoth N, Rudin M. Structural basis of large-scale functional connectivity in the mouse. J Neurosci 2017; 37: 8092–8101. [PubMed: 28716961]
59. Shofty B, Bergmann E, Zur G, Asleh J, Bosak N, Kavushansky A et al. Autism-associated Nf1 deficiency disrupts corticocortical and corticostriatal functional connectivity in human and mouse. Neurobiol Dis 2019; 130: 104479. [PubMed: 31128207]
60. Asleh J, Shofty B, Cohen N, Kavushansky A, López-Juárez A, Constantini S et al. Brain-wide structural and functional disruption in mice with oligodendrocyte-specific Nf1 deletion is rescued by inhibition of nitric oxide synthase. Proc Natl Acad Sci U S A 2020; 117: 22506–22513. [PubMed: 32839340]
61. Loitfelder M, Huijbregts SCJ, Veer IM, Swaab HS, Van Buchem MA, Schmidt R et al. Functional Connectivity Changes and Executive and Social Problems in Neurofibromatosis Type I. Brain Connect 2015; 5: 312–320. [PubMed: 25705926]
62. Yoncheva YN, Hardy KK, Lurie DJ, Somandepalli K, Yang L, Vezina G et al. Computerized cognitive training for children with neurofibromatosis type 1: A pilot resting-state fMRI study. Psychiatry Res - Neuroimaging 2017; 266: 53–58. [PubMed: 28605662]

63. Chabernaud C, Mennes M, Kardel PG, Gaillard WD, Kalbfleisch ML, VanMeter JW et al. Lovastatin regulates brain spontaneous low-frequency brain activity in Neurofibromatosis type 1. Neurosci Lett 2012; 515: 28–33. [PubMed: 22433254]

64. Tajan M, de Rocca Serra A, Valet P, Edouard T, Yart A. SHP2 sails from physiology to pathology. Eur J Med Genet 2015; 58: 509–525. [PubMed: 26341048]

65. Tumurkhuu M, Saitoh M, Takita J, Mizuno Y, Mizuguchi M. A novel SOS1 mutation in Costello/CFC syndrome affects signaling in both RAS and PI3K pathways. J Recept Signal Transduct 2013; 33: 124–128.

66. Du Z, Shen Y, Yang W, Mecklenbrauker I, Neel BG, Ivashkiv LB. Inhibition of IFN-α signaling by a PKC- and protein tyrosine phosphatase SHP-2-dependent pathway. Proc Natl Acad Sci U S A 2005; 102: 10267–10272. [PubMed: 16000408]

67. Ranza E, Guimier A, Verloes A, Capri Y, Marques C, Auclair M et al. Overlapping phenotypes between SHORT and Noonan syndromes in patients with PTPN11 pathogenic variants. Clin Genet 2020; 98: 10–18. [PubMed: 32233106]

68. Gao Y, Shuai D, Bu X, Hu X, Tang S, Zhang L et al. Impairments of large-scale functional networks in attention-deficit/hyperactivity disorder: A meta-analysis of resting-state functional connectivity. Psychol Med 2019; 49: 2475–2485. [PubMed: 31500674]

69. Cortese S, Aoki YY, Itahashi T, Castellanos FX, Eickhoff SB. Systematic Review and Meta-analysis: Resting State Functional Magnetic Resonance Imaging Studies of Attention-Deficit/Hyperactivity Disorder. American Academy of Child & Adolescent Psychiatry, 2020 doi:10.1016/j.jaac.2020.08.014.

70. Gross AM, Wolters PL, Dombi E, Baldwin A, Whitcomb P, Fisher MJ et al. Selumetinib in Children with Inoperable Plexiform Neurofibromas. N Engl J Med 2020; 382: 1430–1442. [PubMed: 32187457]

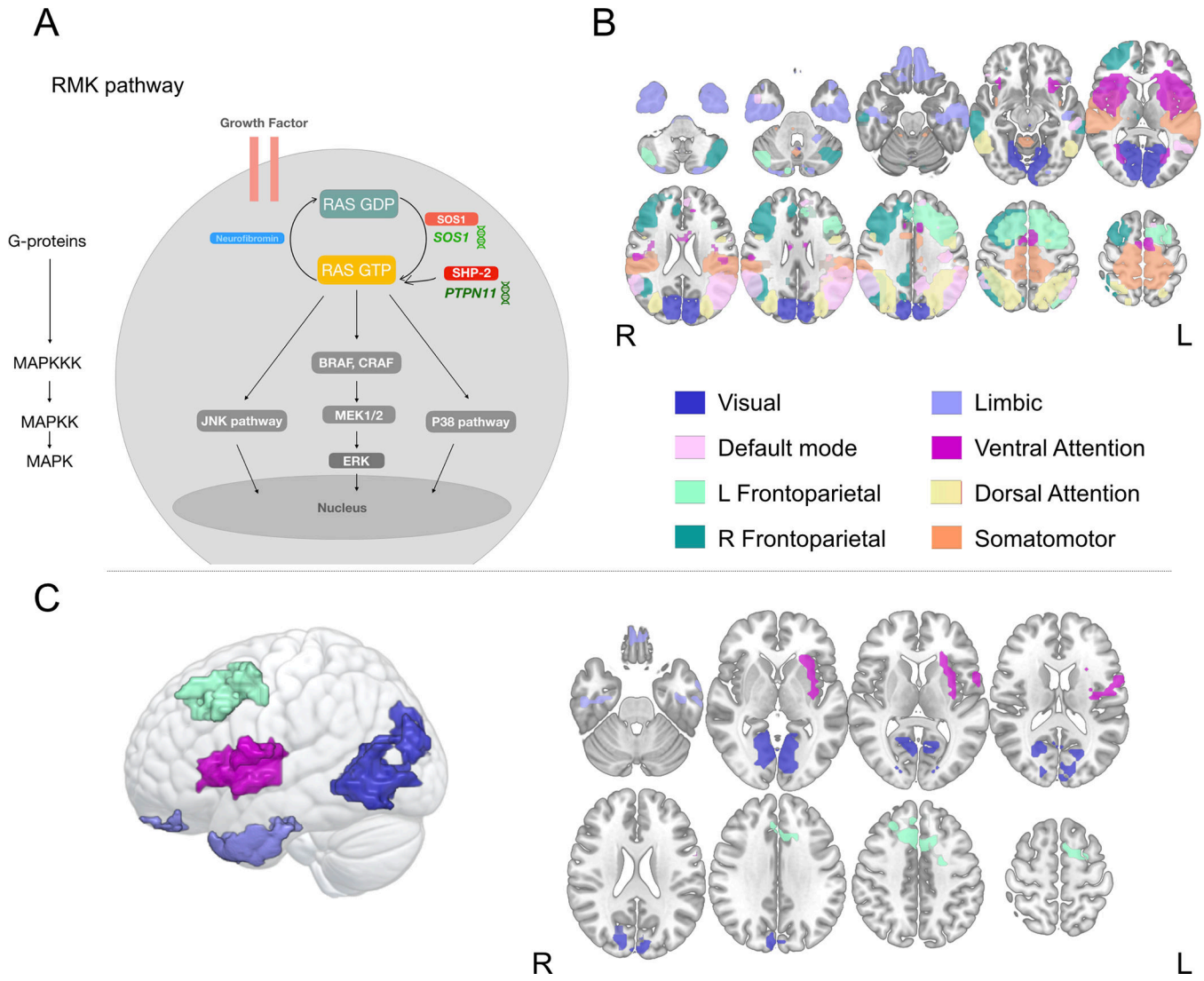

Figure 1.

The Ras/mitogen-activated protein kinase pathway and independent component analysis results.

A. Visualization of key components within the Ras/mitogen-activated protein kinase (Ras/MAPK) pathway. The MAPK pathway consists of three kinases (MAPKKK, MAPKK, and MAPK), which form a signal transduction cascade that receives input from G-proteins and produces different biological outputs. The Ras/MAPK/ERK pathway is illustrated in detail reflecting the two studied genes (*PTPN11* and *SOS1*) and encoded proteins (SHP-2 and SOS1). Two associated pathways include JNK and P38. SOS1 and SHP-2 proteins are displayed in warm colors reflecting their activation of RAS phosphorylation and Neurofibromin in a cold color reflecting loss of inhibition - that also results in pathway activation.

B. Networks identified across groups using independent component analysis (ICA) displayed on axial slices and transparent brains. C. Clusters demonstrating statistically significant hyperconnectivity in children with Noonan syndrome (NS) within visual,

ventral attention, left frontoparietal and limbic, networks ($p<0.05$ FWE and survived FDR correction across eight networks) displayed on transparent 3D rendering (left) axial slices (right). R= right side of image, L = left side of image.

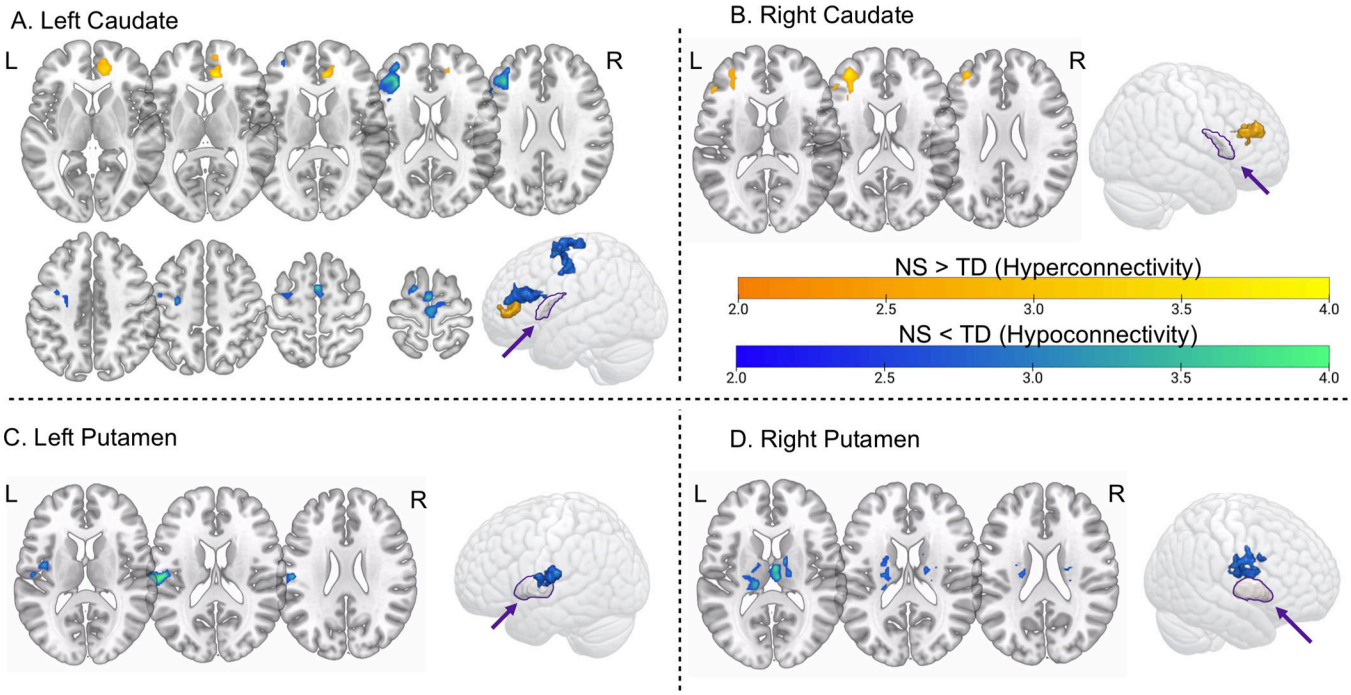

Figure 2.

Seed-based results.

Regions with statistically significant group differences displayed on axial slices. Group differences and seed locations (purple outline and arrow) also shown on transparent 3D renderings. Hot colors represent statistically significant hyperconnectivity in children with Noonan syndrome (NS) relative to typically developing children (TD). Cool colors represent statistically significant hypoconnectivity in children with NS relative to TD. All clusters displayed met the following criteria: Z=2.6, p<0.05 FWE and passed FDR correction for 4 seeds. R= right side of image, L = left side of image.

A

General cognition	PC 1
Narrative Memory Free Recall	-0.274
Picture Puzzles	-0.273
List Memory and List Memory Delayed	-0.269
Comprehension of Instructions	-0.268
Narrative Memory Free and Cued Recall	-0.266
Word Generation Sematic	-0.254
Visuomotor Precision	-0.251
Inhibition	-0.244
NM Free and Cued Recall vs Recognition	-0.24
Imitating Hand Position	-0.237
Memory for Faces	-0.234
Fingertip Tapping Dominant Hand	-0.231
Arrows	-0.215
Affect Recognition	-0.213
Speeded Naming	-0.194
Response Set	-0.189
Memory for faces delayed	-0.177
Naming	-0.125
Auditory Attention	-0.095
Word Generation Initial Letter	-0.049
Fingertip Tapping Nondominant Hand	-0.04
Switching	-0.037

Memory	PC 2
NM Free and Cued Recall vs Recognition	-0.436
Narrative Memory Free and Cued Recall	-0.385
Narrative Memory Free Recall	-0.366
Auditory Attention	0.295
Switching	0.278
Word Generation Initial Letter	0.274
Arrows	0.258
Picture Puzzles	0.247
Memory for faces delayed	0.209
Affect Recognition	0.195
Speeded Naming	0.162
Naming	0.133
Fingertip Tapping Nondominant Hand	-0.12
Word Generation Sematic	-0.089
Memory for Faces	0.072
Fingertip Tapping Dominant Hand	0.071
List Memory and List Memory Delayed	-0.032
Imitating Hand Position	0.032
Visuomotor Precision	0.017
Inhibition	-0.012
Comprehension of Instructions	0.007
Response Set	-0.006

Inhibition/Motor	PC 3
Response Set	0.491
Fingertip Tapping Nondominant Hand	0.474
Switching	0.311
Naming	0.281
Memory for Faces	-0.266
Word Generation Initial Letter	0.254
Speeded Naming	-0.238
Fingertip Tapping Dominant Hand	-0.227
Word Generation Sematic	-0.149
Narrative Memory Free Recall	0.147
Arrows	0.13
Inhibition	-0.096
Memory for faces delayed	0.092
Narrative Memory Free and Cued Recall	0.091
NM Free and Cued Recall vs Recognition	0.075
Comprehension of Instructions	-0.075
Imitating Hand Position	-0.073
Visuomotor Precision	-0.071
List Memory and List Memory Delayed	-0.068
Affect Recognition	-0.029
Picture Puzzles	0.019
Auditory Attention	-0.008

B

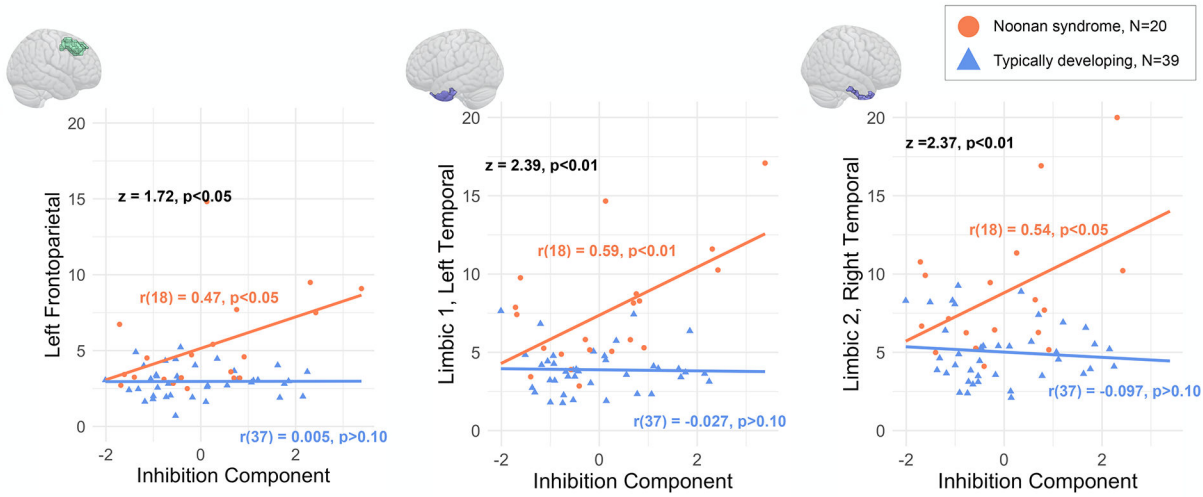

Figure 3.

Principle components analysis and relationships between connectivity and cognition. A. Rotation values and corresponding NEPSY-II scores for the top three components of the principal components analysis (PCA), sorted by absolute value of rotation. Cell color is based on absolute value of rotation for each NEPSY-II score. Rotation values indicate strength of the relationship between the original values (NEPSY=II scores) and the values of a given component. Color is based on the absolute value of rotation (0.5 = dark yellow, 0 = white). B. Relationships between NEPSY-II PCA results and functional connectivity within left frontoparietal, left and right limbic networks. Noonan group in orange and typically developing group in blue. Connectivity values and component scores are in arbitrary units. Brain inlay indicates location of each significant cluster within the corresponding network. Correlation and corresponding p-values are presented for each group (Noonan syndrome in orange and typically developing in blue). Fisher's r-to-z transformation was used, z values

represent comparison of correlation strength between groups and corresponding p-values (in black).

Table 1.

Groupwise descriptive statistics for children included in imaging analysis.

		Noonan Syndrome			Typically developing			Statistical Comparison
		N			N			
N (female)		28 (18)			46 (30)			X2=0.007, p>0.10
Medications	Growth Hormone	8			0			
	Stimulant	2			0			
	Antidepressant	3			0			
	Antipsychotic	2			0			
Tanner Pubic Hair	Stage 1	26			36			X2=3.01, p>0.10
	Stage 2	2			8			
	Stage 3	0			2			
Tanner Breast/ Testicular Development	Stage 1	23			32			X2=2.95, p>0.10
	Stage 2	5			10			
	Stage 3	0			4			
		Mean	Standard Deviation	N	Mean	Standard Deviation	N	Statistical Comparison
Age		8.24	2.16	28	9.07	1.9	46	t(72) = −1.73, p=0.09
FSIQ		95	13	28	112	10	46	t(72) = −6.47, p<0.001
Resting state number frames included		161.4	16.34	28	163.98	14.44	46	U = 604, p>0.10
NEPSY-II subtests								
Motor	Fingertip Tapping Dominant Hand **	8	3	26	11	2	43	U=226.5, p<0.001
	Fingertip Tapping Nondominant Hand **	9	2	25	11	2	43	U=194.5, p<0.001
	Imitating Hand Position **	8	2	27	10	2	41	U=265.5, p<0.001
	Visuomotor Precision **	7	3	28	10	3	45	U=253, p<0.001
Visuospatial	Arrows **	8	4	27	11	2	43	U=307, p=0.001
	Picture Puzzles **	7	3	20	11	3	39	U=136.5, p<0.001
Language	Comprehension of Instructions **	10	2	27	12	2	45	U=325, p=0.001
	Word Generation Sematic **	10	3	28	13	4	45	U= 326, p<0.001
	Word Generation Initial Letter **	7	2	20	10	3	39	U=156.5, p<0.001
Memory	Narrative Memory Free Recall *	10	4	27	12	3	45	U=398, p=0.014
	Narrative Memory Free and Cued Recall **	10	4	28	12	3	46	U=402.5, p=0.006

	Narrative Memory Free and Cued Recall vs Recognition	10	4	24	12	3	41	U=373, p>0.10
	List Memory and List Memory Delayed **	8	3	20	11	3	39	U=190, p=0.001
	Memory for Faces	9	3	27	10	3	43	U=482, p>0.10
	Memory for faces delayed *	9	4	27	11	3	43	U=387, p=0.018
Social perception	Affect Recognition	10	4	28	11	3	46	U=472, p=0.053
Attention and executive function	Speeded Naming *	8	3	26	10	3	45	U=406, p=0.030
	Response Set **	9	3	20	11	2	39	U=173.5, p<0.001
	Auditory Attention *	9	3	26	10	3	44	U=412, p=0.050
	Naming *	8	4	27	10	4	44	U=388.5, p=0.014
	Switching *	9	3	19	11	3	39	U=218.5, p=0.011
	Inhibition **	7	4	27	11	3	44	U=287.5, p<0.001

* significant difference between NS and TD groups

** significant difference between NS and TD groups survives Bonferroni correction for multiple comparisons (within each NEPSY-II domain). FSIQ = Weschler full scale intelligence quotient, Standard scores are presented. NEPSY-II= A Developmental NEuroPSYchological Assessment. Scaled scores are presented. The Visuospatial domain also includes Visuomotor Precision. Resting state data quality (number of frames included in analysis) and some NEPSY-II subtests did not meet assumptions of normality. Therefore, Mann-Whitney U is reported for those variables.

Table 2.

Independent components analysis (ICA) and seed based results.

ICA Network Name	NS vs TD	Cluster index	Cluster Location	Size	p(FDR)	Peak Location (MNI)			SE NS	SE TD	Effect Size			Correlation in NS group
						X	Y	Z			NS vs. TD	PTPN11 vs. TD	SOS1 vs. TD	
Visual	↑	11	bilateral lingual gyrus, cuneus, precuneus	493	0.002	14	−54	−4	1.23	0.56	1.25	1.23	1.69	r(18) = 0.37, p>0.10
Ventral Attention	↑	1	left insula, precentral gyrus, inferior frontal gyrus (pars triangularis), central oppercular cortex	167	0.002	−26	22	4	0.43	0.13	1.28	1.3	1.89	r(18) = 0.40, p=0.087
Left Frontoparietal	↑	1	bilateral anteror cingulate/ paracingulate, superior frontal gyrus	298	0.002	10	22	36	0.58	0.16	1.14	1.03	2.37	r(18) = 0.47, p<0.05[2,4]
Limbic	↑	3	left anterior inferior temporal gyrus, temporal pole, fusiform cortex	159	0.002	−54	−6	−40	0.63	0.21	1.37	1.36	2.03	r(18) = 0.59, p<0.01[3,5]
		2	right temporal pole, fusiform cortex	98	0.002	30	14	−44	0.92	0.29	1.34	1.29	2.28	r(18) = 0.54, p<0.05[3,6]
		1	medial frontal cortex	32	0.009	6	46	−28	0.75	0.13	1.11	1.24	1.76	not tested
Seed location	**NS vs TD**	**Cluster index**	**Cluster Location**	**Size**	**p(FDR)**	**Peak Location (MNI)**			**SE NS**	**SE TD**	**Effect Size**			
						X	**Y**	**Z**			**NS vs. TD**	**PTPN11 vs. TD**	**SOS1 vs. TD**	
Left Caudate	↓	31	left dorsolateral prefrontal cortex, inferior frontal gyurus, pars triangularis BA 45, 44, frontal pole	507	0.002	−32	28	18	0.02	0.01	−0.96	−0.92	−1.35	
		2	bilateral premotor	367	0.011	2	2	62	0.06	0.03	−0.9	−0.75	−1.78	
		11	left premotor/ superior frontal gyrus	203	0.041	−16	2	66	0.02	0.02	−1.18	−1.32	−0.59	

	↑	11	right anterior cingulate, paracingulate	270	0.024	10	38	8	0.02	0.02	0.98	1.02	0.94	
Right Caudate	↑	11	left inferior frontal gyurus, pars triangularis BA 45, 44, frontal pole	270	0.024	−32	44	20	0.03	0.01	1	0.82	2.12	
Left Putamen	↓	11	secondary somatasensory cortex. Parietal opperculum	314	0.019	−52	−18	18	0.02	0.01	−1.32	−1.29	−1.6	
Right Putamen	↓	1	right thalmus	278	0.024	4	−8	10	0.01	0.01	−0.99	−0.67	−2.05	
		2	left thalamus	230	0.041	−14	−28	10	0.03	0.01	−1.43	−1.22	−2.77	

↑Indicates hyperconnectivity in the Noonan syndrome (NS) vs the typically developing (TD) group. ↓ Indicates hypoconnectivity in the Noonan syndrome (NS) vs the typically developing (TD) group. Size = voxels. SE = Standard error of connectivity values for each group based on peak of activation.

[1] Indicates correspondence in PTPN11 subgroup results. A significant cluster in a similar location was found for PTPN11 vs typically developing children. Effect sizes are Cohen's d, calculated for each genetic subgroup (*PTPN11* and *SOS1*) based on each significant peak identified in the primary results. Correlation values for a given cluster with the inhibition/motor component from the principal component analysis (PCA) for the Noonan syndrome group are presented. No correlations were significant within the typically developing group.

[2] Correlation was significant in the Noonan syndrome group

[3] Correlation was significant in the Noonan syndrome group after correcting for multiple comparisons using false discovery rate (FDR). Group difference in correlation strength was calculated for clusters which demonstrated a significant correlation within the NS group.

[4] Group difference in correlation strength was significant ($Z=2.39$, $p<0.01$).

[5] Group difference in correlation strength was significant ($Z=2.37$, $p<0.01$).

[6] Group difference in correlation strength was significant ($Z=1.72$, $p<0.05$).